Şehmus Güden

Engineer
TOFAŞ Turkish Automobile Factory Inc.
Turkey

Ali Riza Motorcu

Professor
Çanakkale Onsekiz Mart University
Faculty of Engineering
Turkey

Murat Yazıcı

Professor
Bursa Uludağ University
Faculty of Engineering
Turkey

Examining and Optimizing the Weld Area and Mechanical Performance of Thermoplastic Parts Manufactured by Additive Manufacturing and Welded by Friction Stir Welding

This study presents an experimental investigation into the weldability of ABS M30 (acrylonitrile butadiene styrene) plates produced by Additive Manufacturing (AM) using Friction Stir Welding (FSW). The effects of FSW process parameters on the yield stress and their optimal levels were determined using the Taguchi method. The optimal welding parameters were found to be a 16 mm tool shoulder diameter, 800 rpm tool rotation speed, and 10 mm/min traverse speed. The weld area of each sample welded using FSW was examined at a macroscopic level. The direction of tool rotation significantly affects the quality and strength of the FSW. When the FSW was performed with a clockwise rotation of the welding tool, a perfect weld could not be achieved. The tunnel effect resulted in gaps in the weld area of the samples at high rotation speeds. Differences were observed in the density between the weld area of the samples and the main parts.

Keywords: Additive manufacturing, Friction stir welding, Thermoplastics, Taguchi method, Yield stress, Acrylonitrile butadiene styrene

1. INTRODUCTION

Additive manufacturing (AM) is a method in which three-dimensional parts can be produced simultaneously by extruding the material in the form of powder, filament, or resin and by casting or curing layer by layer with a laser beam or UV light [1, 2]. The AM method allows for the production of very complex parts without incurring additional costs, and these parts can be assembled directly or with ease. Furthermore, the AM method can reduce the number of parts in a product composed of multiple components [3–5]. The advantages of additive manufacturing (AM) include its ability to produce low-volume products quickly, its toolless manufacturing paradigm, and its ability to meet the demands of high-temperature-resistant engineering polymers. Thermoplastic and polymer components have some mechanical and metallurgical advantages over metal components. Polymers have high corrosion and impact resistance properties [1, 6]. Polymers can be combined with distinct and similar polymer composites, depending on factors like glass transition temperature and rheological characteristics [7]. They have been in high demand in recent years because they are light and easily shaped, and the usage areas of thermoplastics are very common [1–3, 7–9]. For end-product applications, high-temperature polymer parts produced by AM are used in the automotive, biomedical, and aerospace fields [1]. Pro–ducing polymer parts in low quantities using traditional manufacturing processes increases production costs. On the other hand, large thermal gradients, interlayer adhesion, and the printers' inability to reliably maintain the necessary high processing temperatures pose major challenges for AM processing of these polymers [10]. The material extrusion method is generally used to manufacture parts with AM. The material extrusion method is divided into two: fused deposition modeling (FDM) and rod manufacturing (BDM) [1–5]. The AM method uses polymers to produce test samples perfor–med as a single piece (1 piece or a very limited number) [7]. When review studies in the literature are examined, polymers [4, 11–13], high-temperature polymers [10], functional polymers [12], polymer mixtures [12], shape memory polymers [1], polymer composites [1, 14], and hydrogels [12]. Nanocomposites [1], heat-sensitive ma–terials [1], and thermoplastic aliphatic polyesters [2] are used in AM processes. In AM processes in the auto–motive industry, the most common materials are acry–lonitrile butadiene styrene (ABS), acrylonitrile styrene acrylate (ASA), polycarbonate, polylactic acid (PLA), polyetherimide, high-impact polystyrene (HIPS), alip–hatic polyamides (PA, Nylon), polyether ether ketone (PEEK), thermoplastic polyurethane (TPU), and among high-strength plastics and polyetherimide (PEI) are used [3, 4]. ABS material is widely used in the automotive industry due to its strength values and cost [15]. ABS is also common in additive manufacturing [4, 5]. How–ever, research on the FSW of ABS M30 materials produced by additive manufacturing in the literature is limited, and research is ongoing. It is impossible to produce large parts simultaneously with normal AM machines. Therefore, parts are produced in several

pieces for large production and then fixed together. Various joining methods, such as heat plate welding, adhesives, mechanical fixings, etc., are used to fix these parts together. Today, as the impacts of global warming continue to rise, it is crucial to utilize recyclable materials that do not emit harmful gases into the envi–ronment for joining purposes. FSW is an environ–mentally friendly, pollution-free, highly maneuverable, low-energy, and cost-effective welding method [16–19]. Therefore, FSW is becoming a common and popular joining technique due to its increasing potential appli–cations in aerospace, automotive, and other structural industries [20–22]. FSW is a joining in which a non-consumable, rotary-type tool is placed between the interfaces of two plates and is made by friction through rotation at the plate interfaces and by diffusion with heat and pressure [23–25]. FSW is a complex solid-state joining technology that involves temperature, mecha–nics, metallurgy, and interaction [16, 19, and 25]. In the FSW joining process, the weld zone occurs during the progress of the welding tool along the welding path [26]. The welding tool, designed for welding, receives rotational and traverse movements from the milling machine, applying force to the part as depicted in Figure 1. Tool development for FSW processes is an important research topic where studies are ongoing. Another important aspect of the FSW process is the welding tool's design [19, 27]. Therefore, the development of various FSW tools has been considered in recently pub–lished literature [18, 24, 28–31]. The rotation direction generally varies depending on the tooth's direction. The shoulder is the part of the welding tool that contacts the part surface. The pin enters between the two parts and provides friction. The welding path is the joining line of two parts, and welding is done along this path. The main part is one of the parts to be welded, and it indicates the region of the parts that is not affected by heat, as shown in Figure 1. The Heat-Affected Zone (HAZ) is the area weakened by heat. Most of the ruptures occur in this region. The recrystallized nugget is the recrystallized region. The thermomechanically affected zone (TMAZ) shows the thermomechanically affected area in the weld region [26].
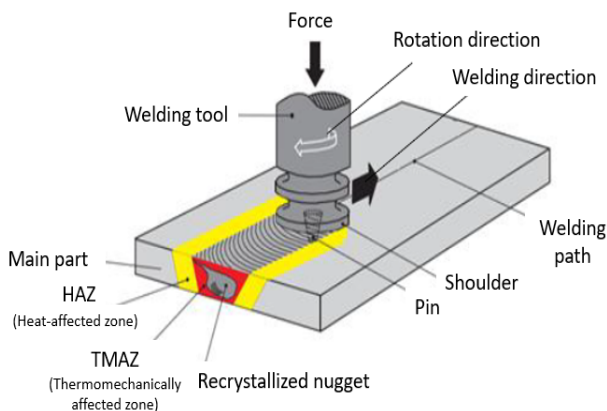
Figure 1. FSW weld zone [26]

In review studies in the literature, tool development in FSW, process parameters and optimization, welding methods, welding of metal and polymer materials [6, 17, 23], joining materials (similar or different), tool

conditions, environmental conditions, joint configurations, and working types [21], the reliability of FSW technologies in repair processes [32], the problems associated with FSW, and the methods developed to overcome these problems [13] have been examined and evaluated in depth. In addition, review studies in the literature have performed in-depth evaluations on the FSW of fiber-reinforced thermoplastic polymers (FRTP) [6, 33], polymer matrix composites, thermoplastic polymers [6, 34], metals [34], and similar and different polymers [6, 35]. Experimental FSW studies focused on polymers [18], dissimilar polymers [29], polycarbonate [7, 36–38], polypropylene (PP) [24, 30, 39, 40], polyethylene [30], high-density polyethylene [27, 40–43], polyamide (PA-6) [41, 43], polyamide (nylon 6) [31, 44], acrylonitrile butadiene styrene (ABS) [28, 38, 45–49], thermoplastic [9, 14], and polyvinyl chloride (PVC) [43]. In these review studies, the effects of different FSW process parameters on tensile stress [32], microstructure [32], hardness [32], corrosion [32], heat generation [33], mixture quality [33], degree of fiber disintegration [33] and, adhesive mechanisms [32, 34] were determined. Several variables affect the mechanical characteristics and quality of FSW weld joints [7]. These factors include FSW process parameters (tool rotation speed, tool inclination angle, tool traverse speed, etc.), tool material, tool geometry (pin profile, pin, and shoulder size, etc.), base material, and environmental conditions (heat-supported tools, tools with cooling support) [7, 42]. In experimental studies in the literature, tool rotational speed [7, 9, 14, 22, 25–28, 37–50], plunge depth [7, 14, 46], dwell time [7, 37, 38, 41], tool traverse speed [14, 22, 24–28, 31, 40, 41, 44–50], tool inclination angle [24], pressure [39], number of passes [41, 47], preheat temperature [41, 49], pin shape [16, 25, 28, 36], mixing time [46], tool diameter [22, 36], tool shoulder diameter [36, 22], axial force [48–50], and tool rotation direction [31] were chosen as control factors (process parameters). Due to the numerous variables involved, optimizing welding conditions is challenging to produce a weld joint with exceptional mechanical properties. However, when optimized, high-quality welded joints with supe–rior mechanical properties and minimal defects are obtained. In experimental studies in the literature, tool spindle torque [18, 24, 36–39], tool forces [18, 24, 29, 30, 36-39], weld morphology [18], tensile strength [18, 19, 24, 28, 30, 39–44, 47, 48, 50], bending strength [24, 27, 39, 41], mixing zone [18, 19, 48, 50], weld quality [18, 49, 50], microhardness [24, 50], weld defects [31, 42], hardness [19, 43, 47], angular distortion [47], weld surface quality [19, 29, 30], joint morphology [38] and residual stress behavior [22] were selected as quality characteristics that determine the mechanical properties and quality of FSW. In addition to parametric-based methods, statistical-based methods are used to deter–mine the effective parameters affecting the FSW weld joint strength. Consequently, for various thermoplastic materials, the ideal ranges of the most efficient process parameters are identified [21]. In FSW research, Tagu–chi Method [7, 11, 38, 40, 41, 51], Box-Behnken, Response Surface Methodology [27, 47], and Full Fac–torial [52, 53] experimental design methods have been

preferred as experimental design and optimization techniques. When the studies in the literature on FSW of thermoplastic materials produced by AM are evaluated, optimized parameters for FSW welding of materials produced by AM must be optimized need to be evalu–ated. These parameters must be determined by consi–dering the material properties and the special requi–rements of the production process. The effect of tooltip design on FSW welding of AM-produced parts still needs to be sufficiently investigated. There is a need for a more in-depth examination of the effects of tooltip design on weld quality and strength. The fact that ma–terials produced by AM generally have a layered structure may affect factors such as density and structural homogeneity in the weld zone in the FSW process. Therefore, the effects of layered structures on the welding process and subsequent mechanical proper–ties need to be investigated.

This study investigated friction stir welding of parts produced by additive manufacturing from ABS M30, a thermoplastic material. Experimental studies were car–ried out to find the optimum levels of FSW parameters. In the study, the mechanical values of the weld area of each test sample welded with FSW were measured, and their behavior was examined with an optical micro–scope. This study is the first pioneering research eva–luating the weldability of thermoplastic polymers with the friction stir technique. This experimental study on the weldability of thermoplastic parts produced by additive manufacturing (AM) with friction stir welding (FSW) will help to provide more information and a comprehensive understanding of the integration of AM and FSW technologies and to understand the structural properties and changes in the weld zone, thus improving the material behavior and performance after welding. It will contribute to the determination of optimized parameters and thus to increasing weld quality and strength and developing reliable and repeatable welding procedures for industrial applications.

2. MATERIALS AND METHOD

This experimental study was conducted in four stages, as illustrated in Figure 2. The first phase is the AM phase with the FDM method. The thermoplastic poly–mer material to be welded with FSW was initially iden–tified during this stage. Subsequently, plates were designed for production, production parameters were determined, and the plates were manufactured using the AM FDM technique.

The second phase is the FSW experiments and optimization of FSW parameters. In this phase, three tool designs were designed and machined on the lathe for use in the FSW experiments. Next, the experimental setup for FSW experiments was established, and the tests were conducted. The third phase of the study con–sists of mechanical tests of FSW-welded parts and experimental studies on the examination of weld zone sections. During this stage, test samples were cut using the abrasive water jet method, followed by conducting tensile tests. The fracture areas of the samples broken by tensile tests were examined at a macro level with an optical microscope. Lastly, the densities of the main parts, filament, and welding area were measured in this phase.

Figure 2. Flow chart of the experimental study

The fourth phase, the last phase of the study, is about evaluating the AM of thermoplastic polymer ma–terials, the FSW process, the tensile test results performed after the FSW process, and the welding area examinations and examining them with the results of literature studies. During this phase, the effects of control factors on the FSW of thermoplastic plates produced using the FDM technique were assessed, and their optimal levels were determined. Following the tensile test, the results of yield stress measurements and the fracture zones of the FSW welded samples were analyzed. Finally, the densities of the main plates and weld regions were compared. Consequently, through this experimental study conducted in four consecutive phases, various aspects, including the AM of ABS-M30 thermoplastic plates using the FDM technique, weldability with the FSW process, the effects of process parameters, the strength of welded plates (via tensile testing), fracture zones of welded areas subjected to tensile stress, and densities were investigated comprehensively.

2.1 Design of ABS M30 test plates and manufactu– ring with FDM technique

Thermoplastic composite samples intended for welding using the FSW technique were fabricated using the FDM-type additive manufacturing method. To create the plates, their dimensions and quantity were specified. Designs were created, and the codes were uploaded into the three-dimensional layered manufacturing device in STL format. The required number of parts for each FSW welding experiment and the number of tensile test samples needed were determined, along with the plate dimensions and quantity. At least nine experiments are required to determine the optimum levels of the welding parameters with the values selected according to the L9 orthogonal array. For each experiment, a pair of FDM-produced ABS plates were utilized, resulting in a total of 18 plates produced for nine experiments. A minimum of 22 plates must be produced to determine the mechanical properties of the welded plates and conduct verification tests. In this study, 40 pairs of plates were fabricated for FSW experiments, resulting in a total of 80 plates being produced.

Tensile samples were designed with the "Siemens NX Continuous Release" software, taking the tensile test sample geometry in the EN ISO 527–2 standard as a reference. The technical drawing of the tensile sample is given in Figure 3 [54]. The thickness of the plates produced is 5 mm.
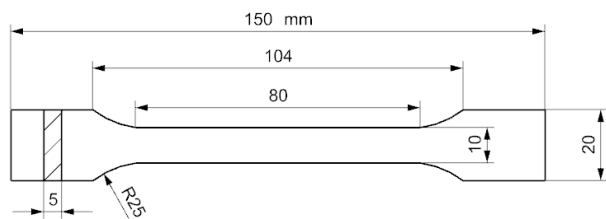
Figure 3. Geometry of tensile test bar specimen

The tensile sample geometry was designed accor–ding to EN ISO 527-2 with dimensions of 150x20x5 mm (Figure 4). It has been determined that five samples

can be obtained from each pair of plates. Therefore, the plates are designed with dimensions of 180x165x5 mm. A pair of plates was utilized for each experiment, as illustrated in Figure 4.
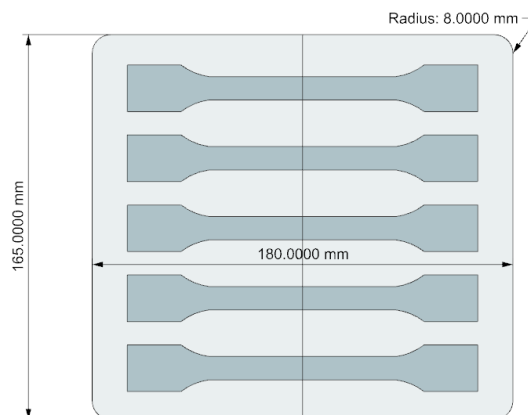
Figure 4. Geometry of ABS plates manufactured with FDM.

Figure 5 depicts the CAM simulation illustrating the tool path movements during AM printing. The plates were manufactured using the FDM technique with a Stratasys Fortus 400 MC model AM device. In the FDM production technique, production is accomplished by melting the material and adding it layer by layer [55]. During this stage, ABS M30 filaments are melted at the crystal melting temperature (Te) [15]. Production com–menced on the table at a lower temperature, following the pattern previously defined by the program. The device has been well calibrated to melt the material well, the temperature of the cast plate to cool the mate–rial gradually, and excellent production has been achi–eved. Fortus 400 MC can produce many high-requi–rement thermoplastic parts such as, ABS-M30™, PC, PPSF, ULTEM® 9085, Nylon 12™, PC-ABS, and ASA [54]. The printing angle is set to 135° at the printing. The device used was calibrated prior to printing to en–sure proper knitting of the support material, absence of misalignments or deviations between the layers of the model material, and correct production of the model (test plates) without any errors resulting from such issues.

a)

b)
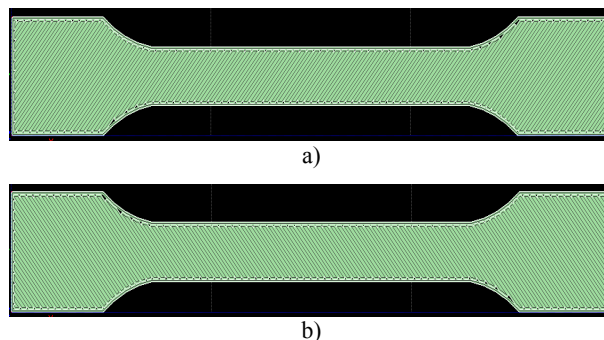
Figure 5. Printing structure with a printing angle of 135°: a) Top view, b) Bottom view

While printing, models were produced from ABS M30 material using a T16-type tip at 190 °C. ABS-M30 belongs to the FDM 3D printing plastics series and is an ideal material for functional prototyping and other 3D printing applications. ABS-M30 stands out with its durability, toughness, lightness, and flexibility. For

general-purpose 3D printing, ABS-M30 is the optimal choice, combining utility and affordability [15]. The glass transition temperature (Tg) of ABS M30 material is 105 °C, and the crystal melting temperature (Te) is 180 °C [48]. The mechanical properties of the material are presented in the following section. During produc–tion, the layer thickness was 0.2540 mm in the Insight 13.7 software settings. Given the inherent anisotropy in layered production, the direction of printing is crucial. In this study, printing was carried out in the XY coordinates. Figure 6 illustrates the 3D-printed plates.
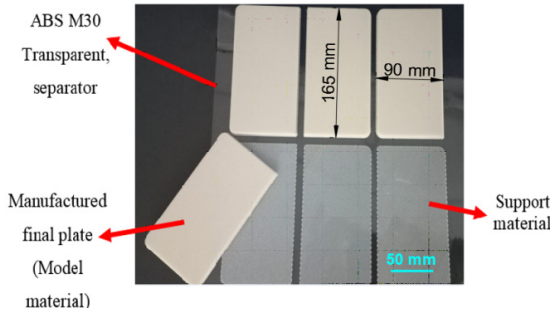
Figure 6. Manufactured final plates

2.2 Selection of levels of control factors and design of experimental study

In order to achieve high strength and a smooth surface in FSW welding, it is crucial to select the correct levels of welding parameters [16]. The heat required for FSW welding depends on various parameter values, such as the shoulder diameter of the welding tool, rotation speed of the tool, traverse speed of the tool, properties of the welding material, penetration depth of the tool, and joint design [16, 22, 25, 26, 50]. The key factors influencing the strength and efficiency of FSW welding are the tool shoulder diameter, tool rotation speed, temperature of the welding zone, and tool traverse speed [23].

In this study, three control factors, identified as most influential on the quality of the FSW process based on the literature, were chosen to investigate and optimize the welding area and mechanical performance of thermo–plastic plates when joining ABS M30 material plates with FSW. These factors are tool rotational speed (S), traverse speed (f), and tool shoulder diameter (d). The rotational speed (S) and traverse speed (f) of the tool are the two primary parameters affecting FSW. The suitable tool rotation speed and tool traverse speed should be selected according to the mechanical and chemical properties of

the material. As the tool rotates, the plasticized material is mixed by the mixing tip and moved from the front to the back of the mixing tip. If the tool's rotation and traverse speed are not selected correctly, the material cannot be transported from the front of the mixing tip to the back. Thus, material accumulation occurs in the welding area in the direction of the tool's rotation or vice versa. The tool rotation speed is the most critical factor for generating welding heat and affects the heat input required for welding [47]. Using a lower tool rotation speed than necessary will not provide sufficient heat, resulting in an inadequate weld [47, 53].

Conversely, employing a higher tool rotation speed than required will increase the fluidity and amount of material in the welding area, making it challenging to control with the tool shoulder [53]. In the study con–ducted by Hajideh et al., it is reported that in the FSW of polyethylene and polypropylene, melting occurs in the main material at high rotation speeds and high tool rotation speeds cause the material to flow out of the weld zone. Additionally, excessively high tool traverse speed values may prevent plasticization of the portion torn off by the tooltip [53].

Another crucial parameter influencing FSW is the tool shoulder diameter. The friction between the mate–rial's upper surface and the tool shoulder generates the majority of the heat needed for welding. Therefore, the size of the tool shoulder is critical in terms of heat generation. The protrusion of the tool shoulder ensures that the heating volume of the material is trapped. The larger the diameter of the tool shoulder part, the more heat will be obtained. Moreover, the pressure applied by the shoulder part prevents the plasticized material from coming out uncontrollably and distorting the shape of the upper surface [26].

According to research in the literature, experiments were conducted within the following ranges: 1000–2800 rev/min for tool rotational speed, 12.5–60 mm/min for traverse speed, 16–24 mm for tool shoulder diameter, and 5–12 mm for pin diameter in the FSW of thermoplastics [11, 15, 21, 53]. Initially, threaded welding tools were utilized in the FSW method [26]. Additionally, in the literature, the tool rotation direction is typically selected as clockwise for the right helical screw [7]. When selecting the levels of control factors, the results and recommendations from the limited number of studies in the literature were taken into con–sideration. Control factors and levels are presented in Table 1.
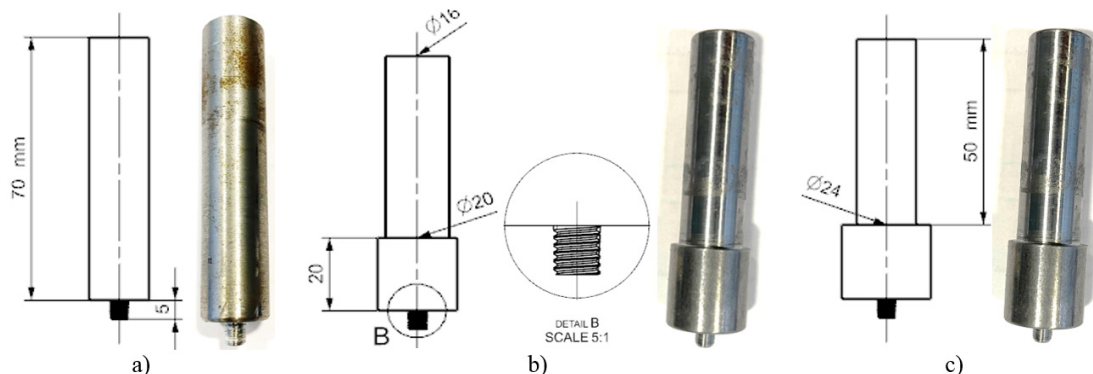
Figure 7. Tools used in the experimental study and their technical drawings: a) Shoulder diameter 16 mm, b) Shoulder diameter 20 mm, c) Shoulder diameter 24 mm

Table 1. Control factors and their levels

Control factors	Symbol	Unit	Level		
			Level 1	Level 2	Level 3
Tool rotational speed	S	rev/min	800	1000	1200
Traverse speed	f	mm/min	10	15	20
Tool shoulder diameter	d	mm	16	20	24

The experimental design based on the L9 orthogonal array is presented in Table 2. Experimental design and analysis were conducted using Minitab 20.0 software.

Table 2. Experimental design according to Taguchi method L9 orthogonal array

Trial No	Tool rotational speed	Traverse speed	Tool shoulder diameter
	S (rev/min)	f (mm/min)	d (mm)
1	800	10	16
2	800	15	20
3	800	20	24
4	1000	10	20
5	1000	15	24
6	1000	20	16
7	1200	10	24
8	1200	15	16
9	1200	20	20

2.3 Tool design and manufacturing for FSW

The tools used in the FSW experiments were designed with an M5 right screw as the tool pin (tip), which was 5 mm in length (Figure 7.a–c). In the research con–ducted by Hajideh et al. [53], investigating the effect of tooltip design on FSW of thermoplastics, it was obser–ved that threaded cylindrical tip tools performed better than other types of tooltips. Hence, threaded cylindrical tips were utilized in this study. Tools with shoulder diameters of 16, 20, and 24 mm were manufactured on a lathe from St37 steel (Figure 7.a–c).

2.4 Experimental setup and FSW

The tools depicted in Figure 7.a-c were utilized for welding ABS M30 plates with FSW in an experimental setup on a Mazak VTC 300C II 3-axis milling machine. To secure the produced ABS M30 plates onto the milling machine, a mold measuring 220x205x100 mm was designed to accommodate the plates (Figure 8-a). The mold, made from polyurethane using layered production, was prepared for use by machining the pocket on the milling machine (Figure 8.b). ABS plates were then placed in the mold, and the mold was affixed to the milling machine table using fishplates (Figure 8-c). According to the Taguchi method L9 orthogonal array experimental design provided in Table 2, CNC codes were generated by conducting CAM processing in the NX program for each experiment. During CAM processing in NX, the entry and exit points of the tool on the plates, as well as the traverse speeds and rotation speeds of the tool, are defined. Subsequently, these codes were post-processed and translated into machine language, and experimental studies were conducted. The direction of tool rotation is defined as counterclockwise due to the utilization of a metric right-hand screw. The FSW welding process is illustrated in Figure 8-d, where two plates are fixed face-to-face for the welding process (Figure 8.d). The tool is then advanced along the line where the surfaces overlap, and welding is performed using the heat generated by friction between the tooltip and the plates. A sample of completed welding is shown in Fig 8.e and f, respectively.
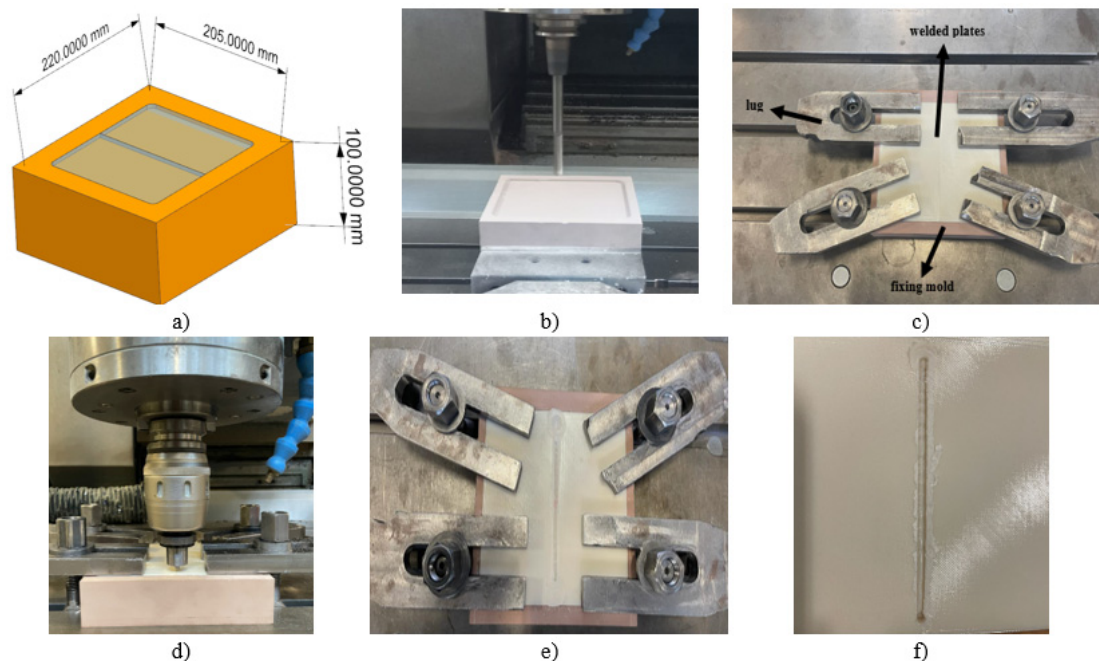
Figure 8. FSW experimental setup: a) Design picture of fixing die, b) Machining the fixing mold on the milling machine, c)Fixing the plates on the milling machine with the help of molds and fishplates, d) Performing FSW welding, e) Plates welded with FSW, f) FSW welded final product

2.5 Abrasive water jet cutting of tensile test specimens

Since ABS M30 is a thermoplastic material sensitive to heat, water jet cutting was chosen for cutting the tensile test samples from the plates to ensure a smooth cut without damaging the material's structure. ABS M30 plates were subjected to FSW, and performed in nine different combinations as listed in Table 2. Following the FSW experiments, five samples were cut from each experimental set using an abrasive water jet (Figure 9.a), resulting in a total of forty-five tensile samples. Additionally, three non-welded ABS M30 sheets were produced and cut to determine the strength values of the base material (Figure 9.b). Samples that underwent FSW welding and were subsequently cut with an abrasive water jet are depicted in Figure 9.b.

a)
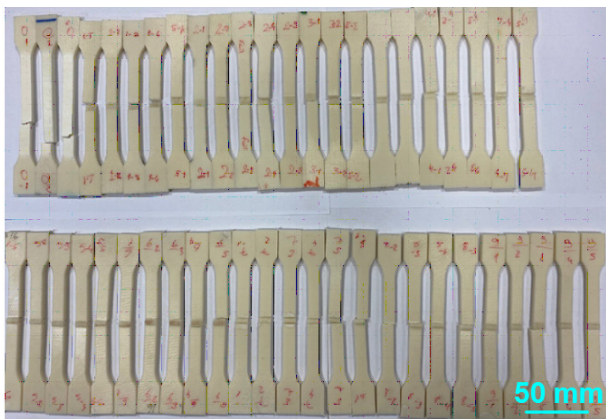
b)

Figure 9. FSW welded and AWJ cut plates for tensile test specimens: a) Cutting 5 samples with AWJ from each experimental set, b) All samples broken/ruptured by tensile test (48 pieces)

2.6 Tests and devices used in examining the weld area

Tensile tests were performed according to ISO 527 standards at 10 mm/min. This test aimed to determine the highest stress value and elasticity modulus of both the unwelded state and the welding area of the ABS M30 material, with a force-displacement graph gene–rated accordingly. An extensometer was employed to measure the displacement value during the tensile test, with tensile stress values reported in the N/mm^2 unit. A Zeiss 50X stereoscope was utilized to examine the weld areas thoroughly. To ensure clear visibility of the weld areas, they were cleaned meticulously using paper sandpaper. Initially, rough processing was conducted with P400, followed by surface smoothing with P800, and finally, a finishing polish with P1500. Density differences between the FDM-produced region and the welding region were measured using a Sartorius brand density measurement scale employing the liquid floo–ding method, with ethyl alcohol serving as the liquid in this scale.

3. RESULTS AND DISCUSSION

In this section, the experimental findings obtained in the examination and optimization of the weld zone and mechanical performance of thermoplastic parts resul–ting from the experimental study carried out according to the experimental pattern in Table 2, at the levels of control factors given in Table 1, with FSW welding of plates produced using the FDM technique, are pre–sented and discussed.

3.1 Evaluation of the effects of FSW parameters

The effects of constant parameters in FSW (e.g., tool rotation direction) and variable parameters (control factors, e.g., tool shoulder diameter, tool traverse speed, tool rotation speed) on the weld zone and mec–hanical performance of welded thermoplastic plates were evaluated in this section.

3.1.1. Tool rotation direction

As a result of the preliminary experiments, it was seen that the direction of tool rotation has significant effects on FSW quality and strength. As can be seen in detail from Figure 10.a, since the screw drilled into the cylindrical pin is a right screw, the screw helix angle increases from the right to the top. It has been determined that the most important thing to consider when choosing the direction is to ensure that the liquid polymer material melted during friction moves inward to fill the welding mouth and weld line with the rotation moment applied by the tool. This result was obtained in preliminary experiments when counter–clockwise (CCW) rotation was applied with right-hand helix tools (Figure 10.b). In the FSW application, which was carried out by rotating the tool clockwise (CW), it was observed that the melted material moved away from the welding lip and line, and therefore, the joining could not be achieved (Figure 10.c). In clockwise FSW, the materials abraded by the tool broke away from the surfaces of the plates without fusing and moved with the tool, depending on the width of the tool's shoulder diameter and the tool rotation speed (Figure 10.d). Therefore, all FSW tests were carried out within a counterclockwise tool

rotation direction. Research by Gao indicated that in the FSW of PA6 material, a left-threaded pin profile with counterclockwise rotation or a right-threaded pin profile with clockwise rotation results in a well-welded zone with desirable properties [17]. Similarly, it has been reported that when joining Nylon 6 plates using FSW with a threaded pin profile, a left-threaded pin profile rotating counterclockwise or a right-threaded pin profile rotating clockwise produces a satisfactory welded area with desirable properties [31].
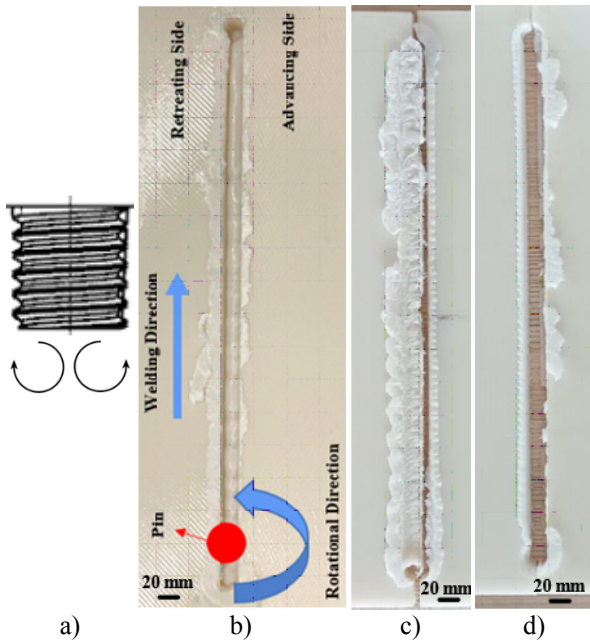
Figure 10. Right helical threaded pin, tool rotation direc– tions, FSW welding zones when the tool rotation direction is clockwise (CW) and counter clockwise (CCW): a) Right helical threaded pin, tool rotation directions, b) Successful welding result in tool rotation direction CW, c) In CW tool rotation direction, the melted material moves away from the welding belt, d) The traverse movement of the tool by removing material from two plates in the tool rotation direction CW

It was determined that the welding direction should be illustrated in Figure 11, which was utilized for all experiments. Additionally, the advancing side can be designated as the edge where the tool penetrates the material, while the retreating side can be identified as the edge where the torn material is accumulated.

3.1.2. Tool rotational speed and traverse speed

In preliminary experiments carried out with high tool rotation speeds (S=1500–1800 rev/min), FWS welding could not be achieved at all traverse speeds, and it was observed that the material melted only along the tool advance direction. The rotation speed of the tool plays a crucial role in heat generation in both metals and polymers, as asserted by various authors [47, 49, and 52]. As depicted in Figure 11, an increase in the tool rotation speed resulted in increased friction in the con– tact area, leading to expansion in the welding region. It was evident that FSW could not be executed at high tool rotation speeds, prompting further preliminary tests to determine the values at which successful joi– ning could occur. Five additional preliminary tests

were conducted at different levels of tool rotation and traverse speeds while maintaining the tool shoulder diameter at 20 mm (Figure 11.b). Figure 11.b illustrates that in Friction Stir Welding conducted with lower tool rotation and traverse speed, the welding quality appears notably superior at the macro level. Therefore, with six preliminary experiments, it was determined that the FSW parameters given in Table 1 would be most suitable for FSW tests.

a)

b)
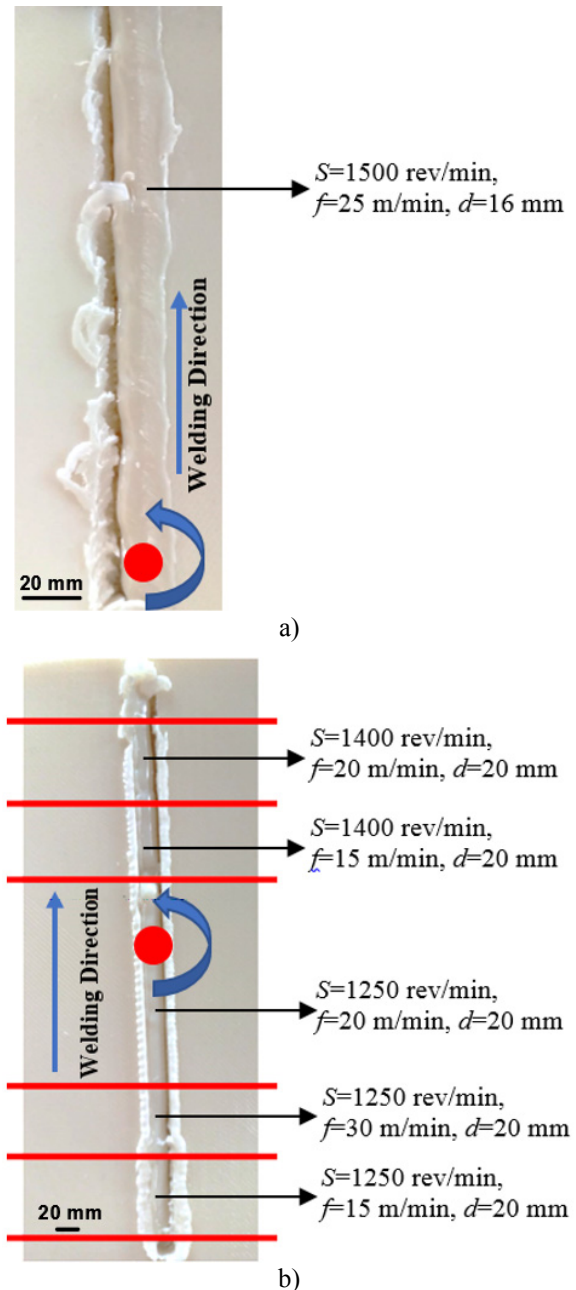
Figure 11. Preliminary tests to determine the levels of FSW welding parameters: a) Expansion of the weld area due to high tool rotational speed (S=1500 rev/min, f=25 mm/min, s=16 mm), b) Welding zones at different tool rotational speeds and traverse speeds

3.1.3. Yield stress results of tensile test

The parts manufactured using ABS M30 material were welded using FSW based on the Taguchi method L9 orthogonal array pattern outlined in Table 2, employing various levels of the FSW parameters indicated in

Table 1. Tensile tests offer insights into the mechanical strength of plastic materials.

Depending on the applied tensile force, the mate–rial's yield stress, percentage elongation, ductility, or brittleness can be determined through the tensile test. As shown in Table 3, the maximum yield stress was measured at 9.80 N/mm², while the minimum yield stress was recorded at 3.17 N/mm².

Table 3. Tensile test results.

Trial No	Tool rotational speed	Traverse speed	Tool shoulder diameter	Yield stress (N/mm²)
	S (rev/min)	f (mm/min)	d (mm)	
1	800	10	16	9.80
2	800	15	20	3.17
3	800	20	24	3.50
4	1000	10	20	4.30
5	1000	15	24	5.85
6	1000	20	16	5.15
7	1200	10	24	5.70
8	1200	15	16	5.50
9	1200	20	20	3.82

The stress-strain graph from the tensile test results was generated using the Zwick Roell Z010 machine TestXpert II software interface (Figure 12). This stress-strain graph, as depicted in Figure 12, corroborates the findings presented in Table 3. The tensile test results of the samples welded with FSW indicate that sample no. 1 (Test no. 1) yielded the maximum yield stress after the application of tensile force, while sample no. 2 (Test no. 2) exhibited the minimum yield stress. Maximum yield stress values were attained within the elongation range of approximately 0.15–0.25% across all samples. Taguchi method analyses were conducted employing the "larger is better" approach to ascertain the effects of FSW parameters on yield stress and to determine the levels of FSW parameters that yield the maximum yield stress.
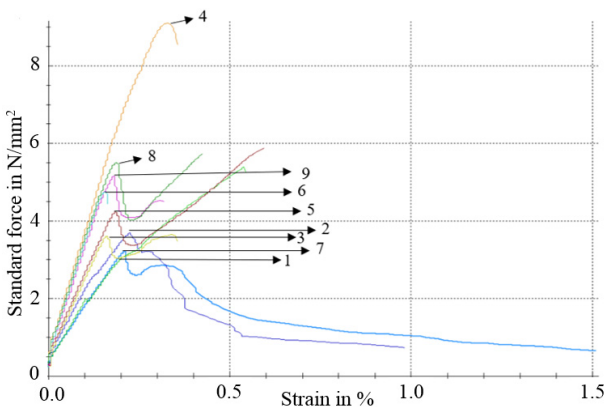
Figure 12. Stress-% strain graph

The main effect graph for yield stress is depicted in Figure 13. As illustrated in Figure 13, the order of the effect of FSW parameters on yield stress is as follows: tool shoulder diameter, tool traverse speed, and tool rotation speed. Lower yield stress values were obser–ved at higher tool rotation speeds and traverse speeds (Figure 13). The reasons for the failure of the FSW

process with high tool rotation speed and traverse speed were explained in Subheading 3.1.2, based on the preliminary FSW experiments conducted within the scope of this study. Hence, this trend observed in the main effect graph aligns with the findings obtained from the preliminary experiments.
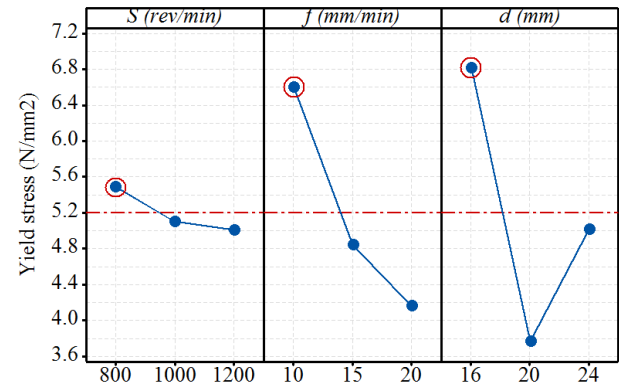
Figure 13. Main effect plot for yield stress

During the FSW process, the tool rotation speed plays a crucial role in both heat generation and material mixing. Given that thermoplastic materials possess low heat transfer capabilities, a substantial amount of heat input is required to soften and mix the material effec–tively. Consequently, defects such as pinholes and tun–nels resulting from inadequate heat input are mitigated by enhancing material flow during the process. As a result, the tensile strength of the welded joint expe–riences a significant improvement. Moreover, the inc–reased heat input facilitates better mixing action and material flow, thereby enhancing the plastic defor–mation of the joint during tensile loading. Conse–quently, the area under the stress-strain curves expands, increasing impact energy [47]. Low tool rotation speeds result in inadequate material flow in the weld zone and a lack of fusion between the weld and the base material.

Additionally, frictional heat increases with tool rotation speed. While higher rotational speeds promote better mixing of the weld material and higher tensile strength, welding at excessive rotational speeds can cause the burning of the workpiece and render the welding procedure uncontrollable [44, 52]. In this study, higher yield stress values were attained at lower tool rotation speeds, and an increase in the tool rotation speed led to a decrease in the yield stress values (Figure 13) [28]. This result indicates that the nece–ssary heat input for achieving the desired weld strength could be attained at a tool rotation speed of 800 rev/min. Tool rotation speed significantly influences the energy generated during the welding process, the–reby serving as a proxy for energy input [49]. It is hypothesized that at higher rotation speeds (1000 rev/min and 1200 rev/min), the elevated heat leads to increased material flow and fluidity in the welding area, making it challenging to control with the tool shoulder, thereby resulting in weaker weld joints. Moreover, excessive melting at very high tool rotation speeds causes the liquefied material in the welding area to be expelled from the weld zone by the tool shoulder, resulting in material loss from the welding area [26]. In

the study by Hajideh et al., it is noted that excessive rotation speeds lead to an additional input of welding heat and high inertia forces, resulting in defects in the mixing zone and consequently weakening the strength of the connection. It is mentioned that higher tool rotation speeds induce turbulent material flow [53]. Rudrapati's research suggests that among other process variables, tool rotation speed exerts the most significant influence, and it is stated that weld quality deteriorates with increasing tool rotation speed [56]. In the FSW of polyethylene plates, burning, plate distortion, and vibration on the tool shoulder were inevitable at high tool rotation speeds. Increased rotation speeds led to elevated process temperatures due to frictional heat, resulting in material burning and emitting a burnt smell during the process [27]. Similarly, in the FSW of ABS, high tool rotation speeds caused an increase in process temperature (friction-induced heat), resulting in burns and peeling on the workpiece surface [52].

High tool traverse speeds reduce tensile strength and result in poor material mixing. In samples with higher tool traverse speed, weld line deflection and deformation occur, leading to inadequate material mixing and, consequently, lower tensile strength. It is seen in the literature that choosing the tool traverse speed as high as possible does not cause any problems in welding quality. However, higher tool traverse speeds prevent the rotary pin from heating the weld area for a longer time [44, 52]. In this study, higher yield stress values were obtained at lower tool traverse speeds (Figure 13) [43]. The lower yield stress values observed at higher tool traverse speeds were attributed to incomplete plasticization of the material removed by the tooltip, particularly noticeable at traverse speeds of 15 mm/min and 20 mm/min. Consequently, weaker weld bonds were formed at higher tool traverse speed settings. Tool traverse speed can be regarded as the rate of energy transmission from the tool rotation speed to the polymer. It can be inferred that lower traverse speeds result in higher heat input to the weld [49]. In this study, the adequate welding heat input achieved at a tool traverse speed of 10 mm/min ensured sufficient fluidity in the mixing zone, resulting in a uniform welding area [53]. As mentioned in the study by Mendes et al., higher traverse speeds result in more forced material flow, which hinders material mixing. Consequently, the adhesion of the polymeric material to the retreating side is reduced, promoting the formation of defects in this region [49]. Conversely, excessively low tool traverse speed prolongs welding time and reduces process efficiency. Therefore, low traverse speed is avoided in FSW applications [52]. This study determined the optimum traverse speed as 10 mm/min. Although the processing time at this low tool traverse speed is long and, therefore, the efficiency is low, the fact that the highest yield stress strength was obtained at this traverse speed compared to other conditions (e.g., at higher tool traverse speeds) causes the importance of long processing time and efficiency to be ranked second.

In this study, maximum yield stress strength was obtained when welding 5 mm thick ABS M30 thermoplastic plate materials with tools with a shoulder

diameter of 16 mm. The effect of tool shoulder diameter on weld strength and appearance is significant. Most of the heat in the welding area is generated from the friction between the shoulder part of the welding tool and the upper surface of the workpiece. This positive welding result in terms of strength is attributed to sufficient heat in welds made with 16 mm shoulder-diameter tools. Lower yield strength values were obtained in the experiments conducted with welding tools with 20 mm and 24 mm shoulder diameters, and the lower yield strength results were attributed to the formation of a weaker weld bond due to the difficulty in material flow in the welding area.

The mean response results for yield stress are presented in Table 4. The differences between the levels of each FSW parameter indicate the degree of impact of each parameter. A significant difference between the levels of an FSW parameter suggests that the effect of that parameter is substantial. Accordingly, supporting the main effect graph in Figure 13, the order of influence of FSW parameters on yield stress is tool shoulder diameter, traverse speed, and tool rotation speed. The average response table also determined the optimal levels of FSW parameters. In order to obtain maximum yield stress strength in the welding area of parts produced by additive manufacturing from ABS 30 material and to be welded with FSW, a tool with a shoulder diameter of d = 16 m and welding parameters S = 800 rev/min, f = 10 mm/min should be used. In the study conducted by Gao et al., it is mentioned that process parameters such as tool traverse speed, pressure time, tool rotation speed, and pin diameter affect the flow stress and the highest temperature of the welding zone but do not affect the yield stress [17].

Table 4. Mean response table for yield stress

Level	S (rev/min)	f (mm/min)	d (mm)
1	5.490*	6.600*	6.817*
2	5.100	4.840	3.763
3	5.007	4.157	5.017
Delta	0.483	2.443	3.053
Rank	3	2	1
(*) Optimum level			

The statistical significance of the main effects of FSW parameters on yield stress was determined by Analysis of Variance (ANOVA) at a 95% confidence level (P < 0.05). Although the FSW parameters did not exhibit statistically significant effects since their P-values were less than 0.05, a closer examination of the percentage contribution rates of these parameters reveals that the most influential parameter on yield stress is the tool shoulder diameter, accounting for 44.66%, followed by the tool traverse speed with a contribution rate of 30.12%. The effect of tool rotation speed on yield stress remained below 2%. The correlation coefficient (R^2) of the ANOVA was calculated as 0.7603. Since this value is close to 1, it indicates that the model has a high level of confidence. In the study conducted by Hajideh et al., the effects of tool traverse speed and tool rotation speed were found to be almost equal [53]. Azarsa and Mostafapour observed in their study that tool traverse speed had a greater impact than tool

rotation speed [27]. However, in the study by Bagheri et al., it was found that tool rotation speed was the dominant factor in weld strength, with tool traverse speed being the second most effective [52].

Table 5. Mean response table for yield stress

Source	DF	Seq SS	Adj MS	F	P	Cont.%
S (rev/min)	2	0.3944	0.1972	0.05	0.951	1.25
f (mm/min)	2	9.5344	4.7672	1.26	0.443	30.12
d (mm)	2	14.1337	7.0668	1.86	0.349	44.66
Residual Error	2	7.5878	3.7939			23.97
Total	8	31.6503				100.00

3.1.4. Examination of FSW weld area sections

The cross-sectional image of the welding area, taken with an optical microscope at 10 times magnification, is presented in Figure 14. When the cross-sections of the FSW weld region were examined; it was seen that the weld regions in all experiments were similar to those obtained in the literature [26].

a)

A-Zone not affected by heat, B-Zone under the influence of heat, C-Thermomechanically affected zone, D-Recrystallized zone

b)
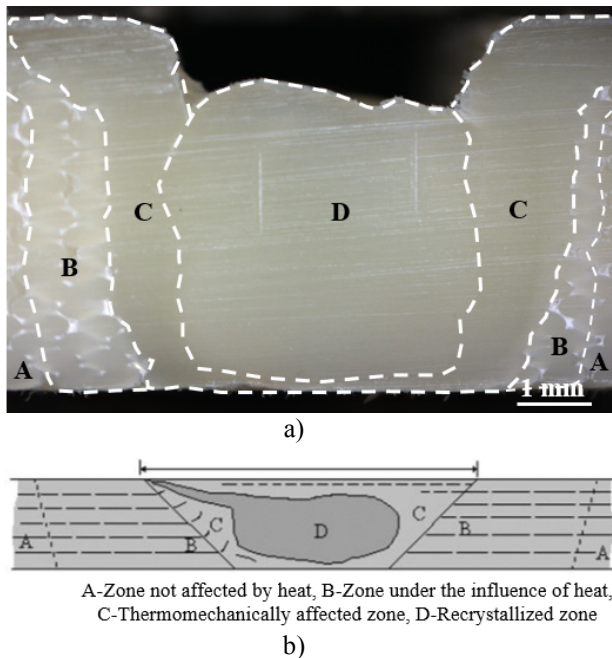
Figure 14. FSW weld zone: a) A cross-sectional photograph of the weld area taken with an optical microscope, b) Schematic representation of the microstructure of the FSW weld zone [26].

Region A, shown in Figure 14, is far from the weld and without deformation. Heat does not affect this region in terms of mechanical properties or microstructure. Region B is the region closer to the weld region. In this region, the microstructure and mechanical properties of the material are affected by the thermal cycle, but plastic deformation does not occur in this region. Region C represents the thermomechanically affected area, where the tool induces plastic deformation of the material. In the recrystallization zone (D), the thermomechanical effect is very severe, and this zone is the center of the weld zone. Intense plastic deformation occurs in the material in this region due to the generated heat [26].

In this study, FSW weld zones of various shapes were obtained under nine different experimental conditions as specified in the experimental set outlined in Table 2. However, mixing regions resembling the one depicted in Figure 14 were generally observed in all experiments, consistent with findings in the literature.

In Figure 15, optical microscope images of the welding areas of three different broken tensile samples (a sample without welds, a sample with minimum stress, and a sample with maximum stress) subjected to a tensile test are provided. When Figure 15 is examined carefully, the most important point that stands out is that in the ABS M30 samples welded with FSW, ruptures occurred from the edge of the welded area or the regions closer to the welded area (A and B areas shown in Figure 14) (see Figure 15.e, f, k, l). This situation is attributed to the fact that the strength of the main plate material is higher than that of the welded area. It is a well-known phenomenon that the breaking strength and stress of welds are typically lower than those of the base material [48]. The findings from the tensile test of the unwelded ABS30 sample and the observations regarding the fracture zone are as follows: The yield strength was measured as 27.5 MPa. During the tensile test, the maximum elongation observed in these samples was 8 mm. A color change was noted in the fractured sample. The elastic modulus (Emod) was found to be 1910.19 N/mm². When viewed from both above and below, the fracture area exhibited a zigzag rupture pattern (Figure 15.a and d). A non-linear rupture was observed when the fracture area was examined from the cross-section (Figure 15.j). Upon juxtaposing the faces of the rupture areas, it was evident that the filaments were arranged in layers (Figure 15.g). Upon inspection of the weld area from above in the sample (Experiment No. 2, S = 800 rev/min, f = 15 mm/min, d = 20 mm), where the minimum yield stress was obtained in the tensile tests, it was observed that melting occurred but did not proceed uniformly (Figure 15.b). Examination of the bottom view of the weld rupture area revealed filaments extending and breaking in a fibrous manner (Figure 15.e). Figures 15 h and k illustrate better welding on the advancing side but less on the retreating side, indicating agglomeration leading to rupture. Figure 15.k reveals an incomplete section, indicating rupture in the heat-affected area.

Conversely, when observing the weld area from above in the sample (Experiment No. 1, S = 800 rev/ min, f = 10 mm/min, d = 16 mm), where the maximum yield stress was obtained in the tensile tests, sequential melting was observed (Figure 15.c). Examination of the bottom view of the weld rupture area showed fiber-shaped structures growing shorter and breaking during rupture (Figure 15.f). The reddish coloring in Figure 15.f results from dust adhering to the hot molten surface, as the part-fixing apparatus is made of polyurethane material. Figure 15.i depicts a wider weld area, while Figure 15.l shows a fuller weld cross-section, with the rupture passing through the heat-affected zone and part of it occurring on the part side. The oval-like structure toward the bottom in Figure 15.l is a result of the pressure exerted by the tool.

The yield stress for the unwelded ABS 30 material was obtained as 27.5 N/mm^2.

The sample in which the minimum yield stress (3.17 N/mm^2) was obtained. Trial No: 2, S=800 rev/min, f=15 mm/min, d=20 mm

The sample in which the maximum yield stress (9.80 N/mm2) was obtained Trial No: 1, S=800 rev/min, f=10 mm/min, d=16 mm
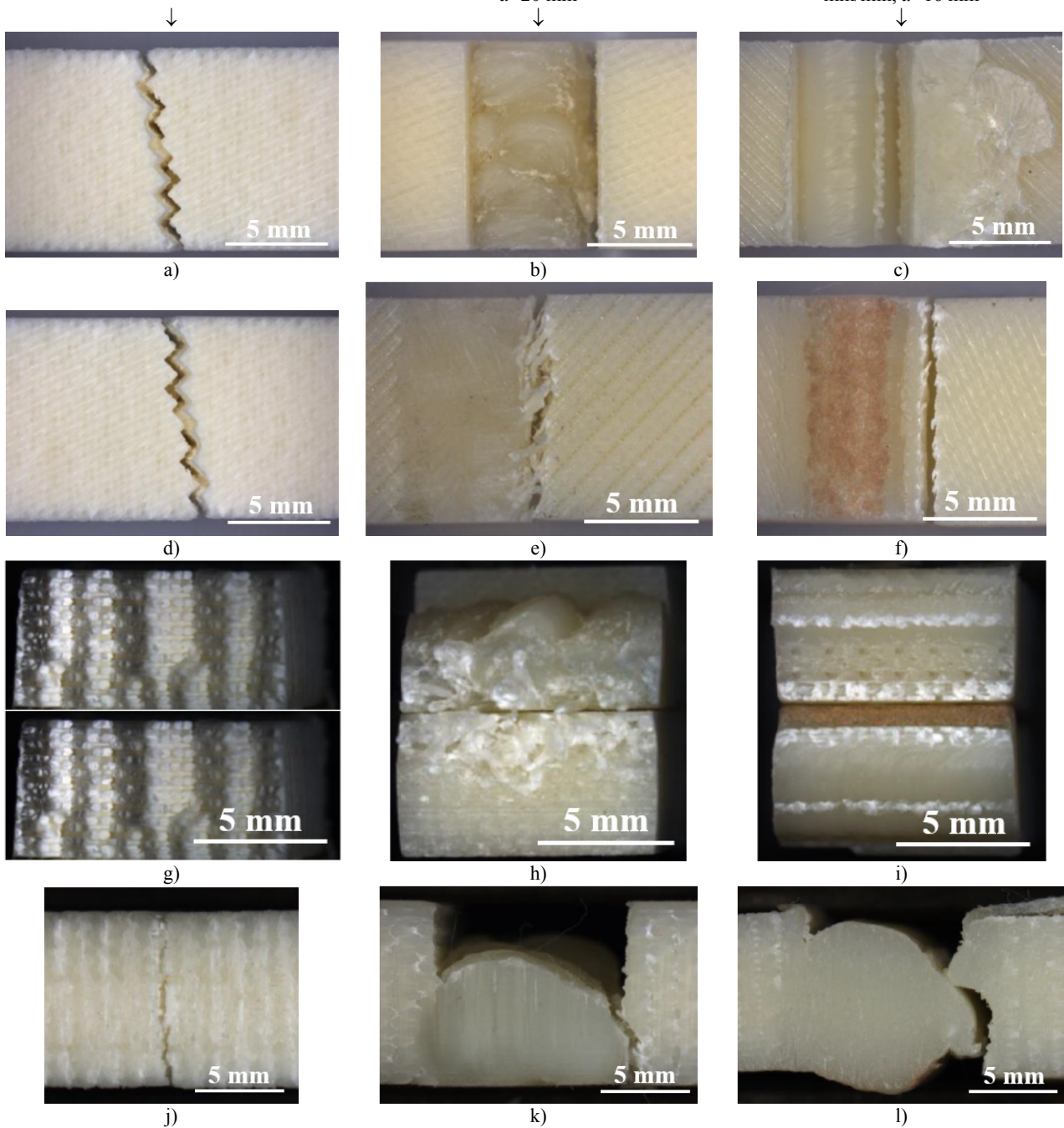
Figure 15. Examination of weld failure areas after tensile stress test: a-c) Top view of the weld rupture area, d-f) Bottom view of the weld rupture zone, g-i) Faces of rupture areas, j-l) Cross-sectional view of the weld area

3.1.5. Comparison of densities of welding area and main thermoplastic plate areas

Figure 16 depicts the cross-sectional view of the welding area. Upon examination of the regions outside the welding zone in Figure 16, the structure of the areas generated by additive manufacturing appears layered and vacuolar, while the weld region appears solid. This raises the question of whether there may be density differences.

Although density is not an effective parameter, it may indirectly affect heat transfer and deformation during FSW [54]. Density differences may cause heat to

be absorbed and dissipated differently during FSW, which in turn may affect the thermal cycle of the FSW process. The mechanical properties of thermoplastic polymer FSW welded joints depend on the density of the welded area [54]. When the welding tool rotates during the FSW process, the polymer chain will move with the direction of rotation of the tool, ensuring perfect filling of the welding area. Therefore, the higher density values measured in the weld area showed that perfect polymer flow was achieved depending on the density of the material. This affected the weld strength as well. As can be seen in the images of the weld rupture zones given in Figure 15, the fact that the ruptures do not occur in the D

region shown in Figure 14 but occur between the A and B regions indicates this.
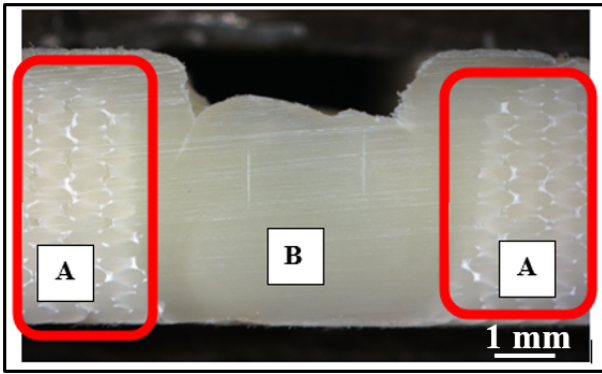
Figure 16. Cross-sectional view of FSW weld area

a)   b)

c)
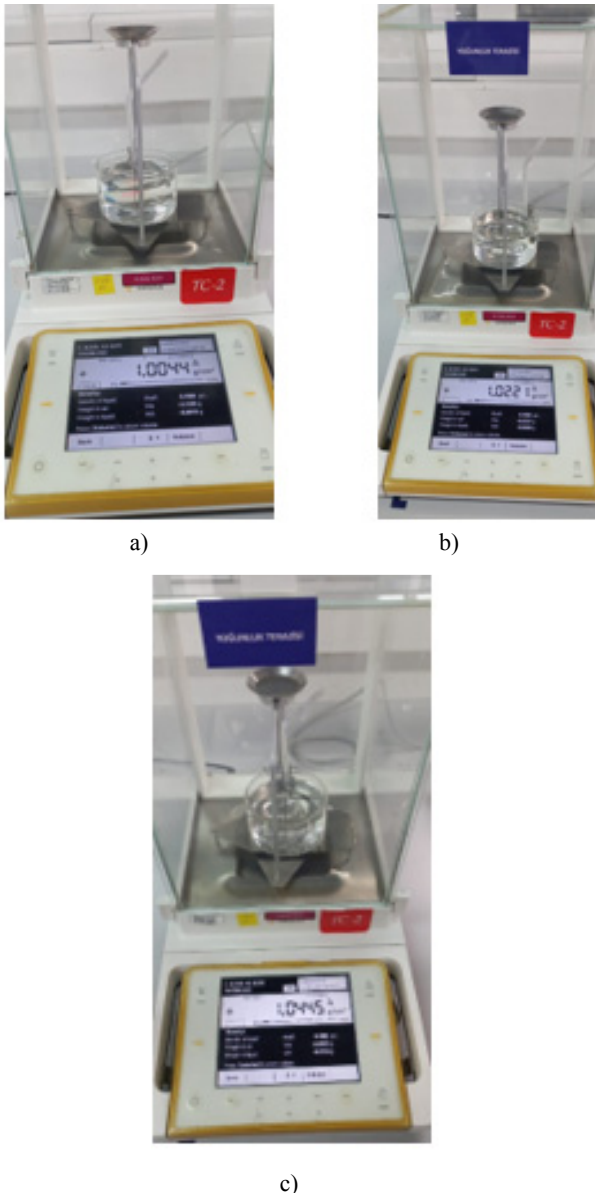
Figure 17. Density measurements of FSW welding area, AM-manufactured ABS M30 part and filament: a) AM-manufactured ABS M30 material, b) Welding region, c) ABS M30 filament

After the tensile tests, a piece of the main material and a weld area of a determined sample were removed with the help of pliers, and their density was measured at 23.5 °C on a density-measuring scale (Figure 17). While the density of the welding area was measured as 1.0221 g/cm^3, the density of the ABS M30 material produced by AM was measured as 1.0044 g/cm^3. The density of ABS M30 filament was measured as 1.0445 g/cm^3 (Figure 17). The technical description document of ABS M30 filament shows its density as 1.05 g/cm^3 when measured at 23 °C according to the ASTM D257 standard. This shows the accuracy of the measurement.

4. CONCLUSIONS

In this experimental study, plates produced by AM from ABS M30 material were welded using the FSW method. Taguchi's experimental design method was employed to determine the optimum levels of welding parameters and the effects of the parameters on the maximum yield strength in the weld zone. Experiments performed according to the L9 orthogonal array were conducted to evaluate the welding strength of ABS M30 plates welded with FSW and compare the welding structure and welding quality. The results obtained after this experimental study are as follows:

1. Tool rotation direction significantly affects the quality and strength of FSW. The most important thing to consider when choosing the direction is to ensure that the liquid polymer material melting during friction moves inward to fill the welding mouth and weld line with the rotation moment applied by the tool. In this study, this behavior was obtained when the direction of rotation was applied counterclockwise in the tool with a right-hand helical screw. In the FSW application performed by rotating the tool clockwise, a perfect weld could not be achieved because the melted material moved away from the welding mouth and line.

2. The optimal levels of control factors for welding ABS M30 material with FSW were determined as follows: tool rotation speed of 800 rev/min, tool traverse speed of 10 mm/min, and tool shoulder diameter of 16 mm. Superior welding quality was achieved in FSW conducted at lower tool rotation speeds and traverse speeds, employing tools with smaller shoulder diameters.

3. It has been determined that the filaments melted in the layers of the main parts in the rupture areas of the samples welded with FSW and, subjected to tensile testing, elongated in the form of fibers and broke. It has been observed that the rupture occurs in the heat-affected area.

4. Gaps were identified in the welding area of samples welded at high tool rotation speeds, attributable to the tunnel effect. Air gaps were observed in the rupture areas of the samples, impacting the weld structure in friction stir welding.

5. The most influential parameters on weld stren–gth (yield stress) were determined to be tool shoulder diameter and traverse speed, while tool rotation speed showed no significant effect.

6. Differences in density were observed between the weld area of the samples and the main parts. The density of the weld zone was measured at 1.0221 g/cm³, while the density of the ABS M30 material produced by ad–

ditive manufacturing was measured at 1.0044 g/cm³. This variance was attributed to the presence of air gaps between layers in additive manufacturing.

As a continuation and complement to this study, consideration is given to exploring double-surface wel–ding or a double-sided tooltip design to enhance the quality and strength of FSW welding for parts manu–factured via additive manufacturing. Additionally, there are plans to bolster the findings of this experi–mental research by incorporating table temperature and tool tip temperature into the FSW parameters under investigation. Furthermore, the welding behavior of various thermoplastic materials produced through additive manufacturing will be analyzed. Optimization of FSW parameters will be conducted, taking into account the types of mesh structures utilized during additive manufacturing.

REFERENCES

[1] Alghamdi, S.S., John, S., Choudhury, N.R., Dutta, N.K: Additive manufacturing of polymer mate–rials: Progress, promise and challenges, Polymers, Vol. 13, No. 5, pp. 1–39, 2021.

[2] Lee, J.Y., An, J., Chua, C.K.: Fundamentals and applications of 3D printing for novel materials, Appl. Mater. Today. Vol. 7, 120–133, 2017.

[3] Chiulan, I., Frone, A.N., Brandabur, C. and Panaitescu, D.M.: Recent advances in 3D printing of aliphatic polyesters, Bioengineering, Vol. 5, No. 1, pp. 1–18, 2018.

[4] Pavlović, A., Šljivić, M., Kraisnik, M., Ilić, J. and Anić, J.: Polymers in additive manufacturing: The case of a water pump impeller, FME Trans., Vol. 45, No. 3, pp. 354-359, 2017.

[5] Sugavaneswaran, M., Thomas, P. M., Azad, A. Effect of electroplating on surface roughness and dimension of FDM parts at various build orien–tations, FME Trans., Vol. 47, No. 4, pp. 880-886, 2019.

[6] Pereira, M.A., Amaro, A.M., Reis, P.N., Loureiro, A.: Effect of friction stir welding techniques and parameters on polymers joint efficiency-A critical review, Polymers, Vol. 13, No. 13, 2056, pp. 1-18, 2021.

[7] Ülker, A., Ayaz, A.: Optimization of process para–meters of friction stir spot welding of polycar–bonate sheets and morphological analysis, Mater–wiss. Werksttech, Vol. 51, pp. 1640–1652, 2020.

[8] Mishra, D., Sahu, S.K., Mahto, R.P., Pal, S.K. and Pal, K: Friction stir welding for joining of polymers, in: Dixit, U.S. and Narayan, R.G. (ed.) *Strengthening and Joining by Plastic Deformation* Springer Singapore, pp.123-162, 2019.

[9] Bindal, T., Saxena, R.K., and Pandey, S.: Analysis of joint overlap during friction spin welding of plastics, Mater. Today: Proc., Vol. 26, No. 2, pp. 2798–2804, 2019.

[10] Das, A., Chatham, C.A., Fallon, J.J., Zawaski, C.E., Gilmer, E.L., Williams, C.B. and Bortner, M.J.: Current understanding and challenges in high temperature additive manufacturing of engineering thermoplastic polymers, Addit. Manuf., Vol. 34, 101218, pp.1-21, 2020.

[11] Mendricky, R., Fris, D.: Analysis of the accuracy and the surface roughness of fdm/fff technology and optimisation of process parameters, Teh. Vjesn., Vol. 27, No. 4, pp. 1166–1173, 2020.

[12] Ligon, S.C., Liska, R., Stampfl, J., Gurr, M. and Mülhaupt, R.: Polymers for 3D printing and customized additive manufacturing, Chem. Rev. Vol. 117, No. 15, pp. 10212–10290, 2017.

[13] Omer, M.A.E., Rashad, M., Elsheikh, A.H., Showaib, E.A.: A review on friction stir welding of thermoplastic materials: recent advances and progress, Weld. World., Vol. 66, pp. 1–25, 2022.

[14] Kumar, R., Singh, R. and Ahuja, I.P.S.: Friction stir welding of 3D printed melt flow compatible dissimilar thermoplastic composites, Proc. Inst. Mech. Eng., Part C., Vol. 235, No. 10, pp. 1878–1890, 2021.

[15] Turku, I., Kasala, S., Kärki, T.: Characterization of polystyrene wastes as potential extruded feedstock filament for 3D printing, Recycl., Vol. 3, No. 4, pp.1-13, 2018.

[16] Kilic, S., Ozturk, F. and Demirdogen, M. F.: A comprehensive literature review on friction stir welding: Process parameters, joint integrity, and mechanical properties, J. Eng. Res., pp.1-9, (Article in press), 2023.

[17] Gao, J., Cui, X., Liu, C. and Shen, Y.: Application and exploration of friction stir welding/processing in plastics industry, Mater. Sci. Technol., Vol. 33, No. 10, pp. 1145–1158, 2017.

[18] Nath, R.K., Maji, P., Barma, J.D.: Development of a self-heated friction stir welding tool for welding of polypropylene sheets, J Braz. Soc. Mech. Sci. Eng., Vol. 41, No. 553, pp. 1–13, 2019.

[19] Sevel, P., Mahadevan, S., Sateš, C., Šrinivasan, D., Džaiganeš, V.: Experimental investigation on the improvement of the properties of the AZ80A Mg alloy joints using friction stir welding process, FME Trans., Vol. 47, No. 3, pp. 452-463, 2019.

[20] Xue, Y., Zhao, H., Zhang, Y., Gao, Z., Zhai, D., Li, Q. and Zhao, G.: Design and multi-objective optimization of the bumper beams prepared in long glass fiber-reinforced polypropylene, Polym. Compos., Vol. 42, No. 6, pp. 2933–2947, 2021.

[21] Iftikhar, S.H., Mourad, A.H.I., Sheikh-Ahmad, J., Almaskari, F. and Vincent, S.: A comprehensive review on optimal welding conditions for friction stir welding of thermoplastic polymers and their composites, Polym., Vol. 13, No. 8, pp. 1-31, 2021.

[22] Sadeghi, S., Karimi, Z. N., Fotouhi, M., Hasani, M., Najafabadi, A. M. and Pavlović, A.: Residual stress evaluation in friction stir welding of aluminum plates by means of acoustic emission and ultrasonic waves, FME Trans., Vol. 46, No. 2, pp. 230-237, 2018.

[23] Kumar, R., Singh, R., Ahuja, I.P.S., Penna, R., Feo, L.: Weldability of thermoplastic materials for friction stir welding- A state of art review and future applications, Compos. Part B Eng., Vol. 137, pp. 1–15, 2018.

[24] Nath, R.K., Maji, P., Barma, J.D.: Effect of tool rotational speed on friction stir welding of polymer using self-heated tool, Prod. Eng., Vol. 16, No. 5, pp.683-690, 2022.

[25] Chakravarthi, G., Giridharan, K., Stalin, B., Pad–manabhan, S., Sekar, S., Nagaprasad, N., Jule, L.T. and Krishnaraj, R.: Investigation on the effect of process parameters on mechanical and microstruc–tural properties of AA8011 similar FSW weld joi–nts, Adv. Mech. Eng., Vol. 14, No. 7, pp.1-16, 2022.

[26] Karagöz, İ.: Properties of friction stir welded thermoplastics, Doctoral thesis, Marmara University, Institute of Science, Metal Education Department, Istanbul, 2014.

[27] Azarsa, E., Mostafapour, A.: Experimental inves–tigation on flexural behavior of friction stir welded high density polyethylene sheets, J. Manuf. Pro–cess., Vol. 16, No. 1, pp. 149-155, 2014.

[28] Pirizadeh, M., Azdast, T., Rash Ahmadi, S., Mamaghani Shishavan, S., Bagheri, A.: Friction stir welding of thermoplastics using a newly de–signed tool, Mater. Des., Vol. 54, pp. 342–347, 2014.

[29] Eslami, S., Ramos, T., Tavares, P.J. and Moreira, P.M.G.P.: Shoulder design developments for FSW lap joints of dissimilar polymers, J. Manuf. Process., Vol. 20, No. 1, pp. 15–23, 2015.

[30] Eslami, S., Ramos, T., Tavares, P.J., Moreira, P.M.G.P.: Effect of friction stir welding para–meters with newly developed tool for lap joint of dissimilar polymers, Procedia Eng., Vol. 114, pp. 199–207, 2015.

[31] Panneerselvam, K., Lenin, K.: Joining of Nylon 6 plate by friction stir welding process using threaded pin profile, Mater. Des., Vol. 53, pp. 302–307, 2014.

[32] Narender, M., Manoj, A., Jakirahemed, M.D.: Stu–dy on defects repairing using friction stir techno–logies, Mater. Today: Proc., Vol. 44, No. 1, pp. 2373–2379, 2021.

[33] Pereira, M.A.R., Galvão, I., Costa, J.D., Amaro, A.M. and Leal, R.M.: Joining of fibre-reinforced thermoplastic polymer composites by friction stir welding - A review, Appl. Sci., Vol. 12, No. 5, 2744, pp. 1-19, 2022.

[34] Sandeep, R., Arivazhagan, N.: Innovation of ther–moplastic polymers and metals hybrid structure using friction stir welding technique: challenges and future perspectives, J Braz. Soc. Mech. Sci. Eng., Vol. 43, No. 7, pp. 1-32, 2021.

[35] Zafar, A., Awang, M. and Khan, S.R.: Friction stir welding of polymers: An overview, In: Awang, M. (eds) 2nd International Conference on Mecha–nical, Manufacturing and Process Plant Engine–ering, Lecture Notes in Mechanical Engineering, Springer, Singapore, pp. 19–36, 2017.

[36] Lambiase, F., Paoletti, A., Di Ilio, A.: Effect of tool geometry on loads developing in friction stir spot welds of polycarbonate sheets, Int. J. Adv. Manuf. Technol., Vol. 87, pp. 2293–2303, 2016.

[37] Paoletti, A., Lambiase, F., Di Ilio, A.: Analysis of forces and temperatures in friction spot stir wel–ding of thermoplastic polymers, Int. J. Adv. Ma–nuf. Technol., Vol. 83, pp. 1395–1407, 2016.

[38] Ülker, A. and Ayaz, A: Joint strength optimization and morphological analysis for friction stir spot welding of the dissimilar thermoplastics ABS and PC, Mater. Test., Vol. 62, No. 11, pp. 1109–1117, 2020.

[39] Nath, R.K., Jha, V., Maji, P. and Barma, J.D.: A novel double-side welding approach for friction stir welding of polypropylene plate, Int. J. Adv. Manuf. Technol., Vol. 113, pp. 691–703, 2021.

[40] Bozkurt, Y.: The optimization of friction stir welding process parameters to achieve maximum tensile strength in polyethylene sheets, Mater. Des., Vol. 35, pp. 440–445, 2012.

[41] Singh, S., Singh, G., Prakash, C. and Kumar, R.: On the mechanical characteristics of friction stir welded dissimilar polymers: statistical analysis of the processing parameters and morphological investigations of the weld joint, J Braz. Soc. Mech. Sci. Eng., Vol. 42, No. 54, pp. 1–12, 2020.

[42] Bilici, M.K.: Investigation of the effects of welding variables on the welding defects of the friction stir welded high density polyethylene sheets, J. Elastomers Plast. Vol. 54, No. 3, pp. 457–476, 2022.

[43] Inaniwa, S., Kurabe, Y., Miyashita, Y. and Hori, H.: Application of friction stir welding for several plastic materials, in: Proc. 1st Int. Jt. Symp. Join. Weld., Woodhead Publishing, pp. 137–142, 2013.

[44] Husain, I.M., Salim, R.K., Azdast, T., Hasanifard, S., Shishavan, S.M. and Lee, R.E.: Mechanical properties of friction-stir-welded polyamide sheets, Int. J. Mech. Mater. Eng., Vol. 10, No. 18, pp. 1-8, 2015.

[45] Kumar, R., Singh, R. and Ahuja, I.P.S.: Repair of automotive bumpers and bars with modified friction stir welding, J. Cent. South Univ., Vol. 27, pp. 2239–2248, 2020.

[46] Kumar, R. Singh, R. Ahuja, I.P.S. and Fortunato, A.: Thermo-mechanical investigations for the joining of thermoplastic composite structures via friction stir spot welding, Compos. Struct., Vol. 253, 112772, pp. 1-17, 2020.

[47] Azhiri, R.B., Sola, J.F., Tekiyeh, R.M., Javidpour, F. and Bideskan, A.S.: Analyzing of joint strength, impact energy, and angular distortion of the ABS friction stir welded joints reinforced by nanosilica addition, Int. J. Adv. Manuf. Technol., Vol. 100, pp. 2269–2282, 2019.

[48] Mendes, N., Loureiro, A., Martins, C., Neto, P. and Pires, J.N.: Effect of friction stir welding parameters on morphology and strength of

acrylonitrile butadiene styrene plate welds, Mater. Des., Vol. 58, pp. 457–464, 2014.

[49] Mendes, N., Loureiro, A., Martins, C., Neto, P. and Pires, J.N.: Morphology and strength of acrylonitrile butadiene styrene welds performed by robotic friction stir welding, Mater. Des., Vol. 64, pp. 81–90, 2014.

[50] Thangaiah, S. I., Sevvel, P., Satheesh, C. and Jaiganesh, V.: Investigation on the impingement of parameters of FSW process on the microstructural evolution and mechanical properties of AZ80A Mg alloy joints, FME Trans., Vol. 46, No. 1, pp. 23-32, 2018.

[51] Kumar, R., Singh, R. and Ahuja, I.P.S.: Friction stir welding of ABS-15Al sheets by introducing compatible semi-consumable shoulder-less pin of PA6-50Al, Meas., Vol. 131, pp. 461–472, 2019.

[52] Bagheri, A., Azdast, T., Doniavi, A.: An expe–rimental study on mechanical properties of friction stir welded ABS sheets, Mater. Des., Vol. 43, pp. 402–409, 2013.

[53] Hajideh, M.R. et al.: Investigation on the effects of tool geometry on the microstructure and the mechanical properties of dissimilar friction stir welded polyethylene and polypropylene sheets, J. Manuf. Process., Vol. 26, pp. 269–279, 2017.

[54] Güden, Ş: Investigation and optimization of the weld zone and mechanical performance of thermoplastic parts which produced by additive manufacturing and welded by friction stir welding Msc. Dissertion, Uludag University, Institute of Science and Technology, Department of Automotive Engineering, Bursa, 2022.

[55] Vorkapić, M., Živojinović, D., Kreculj, D., Ivanov, T., Baltić, M. and Simonović, A. Application of additive technology and reverse engineering in the realization of damaged obsolete parts, FME Trans., Vol. 51, No. 1, pp. 31-38, 2023.

[56] Rudrapati, R.: Effects of welding process conditions on friction stir welding of polymer composites: A review, Compos. C: Open Access, Vol. 8, 100269, pp. 1-7, 2022.

ИСПИТИВАЊЕ И ОПТИМИЗАЦИЈА ПОВРШИНЕ ЗАВАРА И МЕХАНИЧКИХ ПЕРФОРМАНСИ ТЕРМОПЛАСТИЧНИХ ДЕЛОВА ПРОИЗВЕДЕНИХ АДИТИВНОМ ПРОИЗВОДЊОМ И ЗАВАРЕНИХ ЗАВАРИВАЊЕМ ТРЕЊЕМ

Ш. Гиден, А.Р. Моторчу, М. Јазичи

Ова студија представља експериментално истра–живање заварљивости АБС М30 (акрилонитрил бутадиен стирен) плоча које производи Аддитиве Мануфацтуринг (АМ) коришћењем заваривања трењем и мешањем (ФСВ). Методом Тагуцхи утврђени су ефекти параметара процеса ФСВ на напон течења и њихов оптимални ниво. Утврђено је да су оптимални параметри заваривања пречник рамена алата 16 мм, брзина ротације алата 800 о/мин и брзина померања 10 мм/мин. Површина завара сваког узорка завареног коришћењем ФСВ испитана је на макроскопском нивоу. Смер ротације алата значајно утиче на квалитет и чврстоћу ФСВ. Када је ФСВ изведен ротацијом алата за заваривање у смеру казаљке на сату, савршен завар се није могао постићи. Ефекат тунела је резултирао празнинама у зони завара узорка при великим брзинама ротације. Уочене су разлике у густини између површине завара узорка и главних делова.